SPECIFIC GROUND-BASED MONITORING SYSTEM FOR LANDSLIDES ACTIVITY

DRAGOŞ ARMAND STĂNICĂ, DUMITRU STĂNICĂ

"Sabba S. Ştefănescu" Institute of Geodynamics of the Romanian Academy, 19–21, Jean-Louis Calderon St., Bucharest 37, Romania, e-mail: armand@geodin.ro

This paper is centred on the specific ground-based monitoring system used for the assessment of the natural hazard due to both Vrancea's intermediate depth seismic events and the associated Proviţa active fault (PF), which are considered to be the main source of the trigger action of the landslide in Proviţa de Sus locality. In this context, the DC resistivity and high frequency electromagnetic methodologies have been applied and the results highlight the utility of merging the electromagnetic parameters (normalised function Bzn, anisotropy, skewness and strike) and different 2D tomographic images related to post-seismic landslide processes. Subsequently, in the Proviţa de Sus test-site, it was possible to provide information regarding the specific ground motion produced by the interference between external factors and local geotectonic conditions.

Key words: Landslide, earthquakes, active fault, electromagnetic parameters, tomographic images, Proviţa de Sus test-site.

1. INTRODUCTION

Landslides triggered by strong earthquakes caused often most global damages, such as shown by the Khait earthquake (1949, Tajikistan, $M_w = 7.4$), the Peru earthquake (1970, $M_w = 7.7$), the Loma Prieta earthquake (1989, California, $M_w = 6.9$), the Umbria-Marche earthquake (1997, Italy, $M_w = 5.5$), the Chi-Chi earthquake (1999, Taiwan, $M_w = 7.6$), the El Salvador earthquake (2001, $M_w = 7.6$) and Sichuan (2008, China, $M_w = 7.8$).

The rapid development of various techniques and methodologies, such as GPS (Malet *et al.*, 2002), GPS and digital photogrammetry (Mora *et al.*, 2003), correlation of field data with observed instability phenomena (Havenith *et al.*, 2003), high-resolution satellite imagery (Haeberlin *et al.*, 2004), light detection and ranging (McKean, Roering, 2004) and regional patterns of co-seismic landslides (Meunier *et al.*, 2007), as well as spatial distribution of landslides triggered by the earthquakes (Wang *et al.*, 2007) were successfully applied for continuous observation under real field conditions.

Since each landslide involves certain features, it was necessary to choose an adequate monitoring system, on the basis of a preliminary analysis of the studied phenomenon and geological conditions. Thus, the goal of this paper is to present the ground-based monitoring system (GBMS), based on the DC resistivity and high frequency electromagnetic (EM) methodologies, to better understand their efficiency for broad application in landslides hazard assessment (Stănică *et al.*, 2006). Additionally, by combining different data types and analysis techniques, and, also, by merging electric and electromagnetic parameters (normalized function Bzn, anisotropy, skewness and strike) with 2D tomographic images, a landslide model for Proviţa de Sus area is to be realised.

In the end, this paper illustrates the stage of the monitoring system implementation and to what extent the results may contribute to understand the landslide hazard assessment.

2. STUDY AREA AND MONITORING SYSTEM

2.1. Geological settings of the landslide area

In Proviţa de Sus landslide zone, crosscut by deep faults orientated NE–SW, the Proviţa fault (PF) has been reactivated by the intermediate depth earthquakes (Mw = 6) occurred on 27th, November 2004. This earthquake was generated in the north-eastern part of the Vrancea seismic area (45.79N, 26.71E), at 100 km in depth, and the peak ground acceleration (PGA) value recorded at landslide zone was of about 125 $cm.s^{-2}$ (Fig. 1).

This test-site is located in the upper part of the Proviţa Valley, where the ground motion is developed in the flyschoid domain of the Subcarpathians area. The landslide affects the Oligocene formation of the Tarcău Nappe (Moldavides domain), which is characterised by the flyschoid deposits containing slates, sandstones (Fusaru sandstone) and marls. In the studied area there are the Upper Oligocene deposits characterised by the presence of Slon bed – a wildflysch formation which is discordant to the Vineţişu bed consisting mainly of argillaceous marls and thin sandstones. This zone is tectonically very complicated owing to the presence of meso-Cretaceous and Miocene thrusts, and Miocene and post-Miocene faults (Tatu *et al.*, 2005).

This landslide deforms considerably the sliced blocks and produces a complex array of reverse micro-faults, strike-slip micro-faults and folds. Additionally, it is characterised by the following features:

1. the altitudes of front and rear boundaries of the deposits are of 410 m and 670 m;
2. the average slope angle is 18°;
3. the average thickness of landslide deposits – 40 m;
4. the angles of rupture surface are 30° (rear) and 10° (front);
5. the area of landslide deposits is 1.25 km^2;
6. the average volume of landslide deposits – 40 million m^3.

Besides, there are three more important aspects that became the main selection criteria of this landslide as test-site.

1. It is an earthquake-triggered landslide followed by post-seismic slow-slipping ground motion that can be monitored.
2. It is situated nearby Proviţa de Sus locality and can endanger life and property, owing to a high probability of flood, which might be produced by daming Proviţa river due to rockfalls into the watercourse.
3. The existence of logistic base (Geodynamic Observatory Proviţa de Sus) able to supply optimal monitoring conditions and wireless connection with the Center of Bucharest.

2.2. Ground-based monitoring system (GBMS)

One of the main objectives of this paper was to implement a ground-based monitoring system able to provide geophysical data regarding the Proviţa de Sus landslide. This system includes three separate equipments (Fig. 3) able to carry out:

a) continuous monitoring on geomagnetic field in low frequency domain (DC-1 kHz) by using MAG-03DAM system, Bartington-England;

b) discrete observations on:

- electromagnetic field in high frequency domain (0.5 kHz – 24 kHz) by using Geophysical Electromagnetic Measurement System – GMS 06, Metronix-Germany;
- geoelectric field by using Resistivimeter INTEL V3, INTEL92 – Romania;

All three measurement equipments have specific sensors, acquisition modules and adequate software for data processing (Stănică, Zugrăvescu, 2004).

3. METHODOLOGY AND RESULTS

The DC resistivity and high frequency electromagnetic methodologies have been applied in order to carry out the spatio-temporal distribution of the significant parameters for the ground motion occurred on the Proviţa de Sus test-site.

3.1. Distribution of the normalized function Bzn related to the October 27, 2004 seismic event

3.1.1. Theoretical information related to the normalized function Bzn

It is well known that at the Earth surface the vertical geomagnetic component (Bz) is entirely secondary field and its existence is an immediate indicator of lateral inhomogeneity (Word *et al.*, 1970). For two dimensional structures, the Bz is essentially produced by the horizontal geomagnetic component perpendicular ($B_\perp$) to strike and, consequently, the normalized function Bzn defined as:

$$Bzn = Bz/B_{\perp}, \qquad (1)$$

should be time invariant for a given 2D structure in non geodynamic conditions, but it is unstable in geodynamic circumstances and, subsequently, it could be used as a precursory parameter of the seismic activity (Stănică, Stănică, 2007).

In order to define the interrelation between Bzn and electrical conductivity changes, in addition to the relation (1), we may compute the vertical resistivity ρ_z:

$$\rho_z = 0.2\, T \left| E_{\|}/Bz \right|^2, \tag{2}$$

where: T is the period (s) and the $E_{\|}$ is the electric field parallel to strike.

Also, it is possible to write the relation:

$$\rho_{\|} = 0.2\, T \left| E_{\|}/ B_{\perp} \right|^2, \tag{3}$$

where: $\rho_{\|}$ is the resistivity parallel to strike.

Thus, in terms of resistivity the normalized function Bzn may be estimated as:

$$\left| Bzn \right| = (\rho_{\|} / \rho_z)^{1/2} \tag{4}$$

and, subsequently, the normalized function ρ_n may be written:

$$\rho_n = \rho_{\|} / \rho_z \tag{5}$$

The relation (4) demonstrates the fact that the Bzn could be linked to the resistivity/ conductivity variation along the submerged conductive paths (fault systems) through the Earth's lithosphere. Also, the absolute value of the Bzn is able to assess the polarity of the conductivity anomaly (*i.e.*, whether it is more conductive than the surrounding media).

3.1.2. Correlation between normalized function Bzn and earthquakes

Starting with the information regarding the intermediate depth earthquakes (Mw = 6) occurred on October 27th, 2004, which has been emphasized by the daily mean distribution of the normalized function Bzn, carried out by MAG-03DAM monitoring system, it was possible to link the landslide activity occurred in Provița de Sus with this earthquake. Fig. 4 refers to a span of two months (September–October, 2004) monitoring of the normalized function Bzn and emphasizes some anomalous behaviours of the Bzn parameter, having increased values between 1.878 and 1.879. The earthquakes occurred in this interval are marked by vertical lines, with values of magnitude oscillating between 3.0 and 6.0. The maximum value (1.879) of normalized function Bzn, obtained some days prior to EQ of Mw = 6, is related to the resistivity changes due to the stress accumulation and fluids migration along the submerged high sensitive path, deployed at lithospheric level, known as the Carpathian electrical conductivity anomaly (Rokitiansky, Ingerov, 2000).

3.2. Spatial distribution of the electric and high frequency EM data

It is well known that DC resistivity and high frequency EM methods give information about shallow geological structures, presence of fluids and/or conducting meta-sediments, structure dimensionality (2D or 3D), strike direction and spatial distribution of the resistivity.

In order to identify the spatial distributions of the landslide slipping surface and location of the Provița active fault (PF), we carried out 2D tomographic images by using direct current (DC) resistivity method, vertical electrical soundings (VES) version (3.2.1) and high frequency EM measurements (3.2.2).

3.2.1. 2D tomographic images carried out by using DC resistivity method

For the VES version we used the resistivimeter INTEL V3, which is an integrated receiver and transmitter system, and Schlumberger electrodes configuration. The resistivimeter has internal memory of 64 K, sampling rate of 0.2s, output power up to 200 mA, and communication through serial interface enhanced by utility software for Windows XP. To measure the potential difference lead-lead chloride electrodes were used. The apparent resistivities are computed by using the relation

$$\rho_a = k\frac{\Delta V}{I}, \tag{6}$$

where:

$$k = \frac{2\pi}{\dfrac{1}{AM} - \dfrac{1}{AN} - \dfrac{1}{BM} + \dfrac{1}{BN}}$$

is the geometric factor;
where:

– ΔV – the potential difference measured between MN electrodes;

– I – the injected current through the ground by the A and B steel electrodes.

Two resistivity profiles were measured across and parallel to the Provița de Sus landslide. Since the level of non-uniqueness is much more severe in 2D inverse problems and the level of uncertainties in interpretation of the data is also large enough, we made inversion and forward modelling of the resistivity data only for one dimensional case. On the basis of these information the approximate 2D tomographic images (apparent resistivity contours versus depth) are constructed along the both profiles (yellow lines 1 and 2 on the Fig. 2), to obtain the subsurface apparent resistivity distribution and landslide micro-tectonic features (the sliding interfaces depth, cracks and/or micro-faults). Thus, Fig. 5 represents a 2D resistivity image carried out along the landslide zone (yellow line 1) having marked both the sliding surface (white dashed line) and micro-fault (red dashed line), the last one representing the most active landslide rear boundary. The second 2D resistivity image shown in Fig. 6 has been obtained along yellow line 2 on Fig. 2 and shows the signature of both sliding surface (white dashed line) and PF (red dashed line).

3.2.2. 2D tomographic images carried out by using high frequency EM method

Currently, high frequency EM method is a widely used tool in shallow structure investigation since it may provide indication on both the vertical resistivity distribution and micro-fault orientation. Furthermore, the 2D high frequency EM tomographic images in correlation with geological information may provide new insights in the landslide geodynamic activity.

For the high frequency EM data, we have used the Geophysical Electromagnetic Measurement System – GMS 06 for the frequency domain 0.5kHz – 24kHz (Fig. 3). This equipment includes: (i) data acquisition module ADU-06 with 6 channels, GPS-clock, 24 bit resolution and data storage on the internal 440 MB flash disk; (ii) 3 magnetic sensors (induction coils, type MFS06); (iii) 4 electric sensors of Pb-$PbCl_2$.

The MAPROS software packages runs under Windows 95 operating system installed on a laptop which is connected to the data acquisition module ADU-06.

The tasks performed by MAPROS software packages are:

– in-field system calibration and automatic offset compensation;

– real-time data acquisition and processing;

– robust estimation of transfer functions;

– real-time display of time series and all the important EM-parameters.

The data were collected in four stations placed along a linear profile (yellow lines 2, Fig. 2), having 175 m in length and crossing the active fault. The skewness coefficient of the impedance tensor was observed to be less than 0.3 at all the stations in the survey area, and it was assumed that the geoelectric structure is two-dimensional (2D). The impedance tensor was rotated to determine the geoelectric strike and it was found that the lineament pattern is predominantly oriented WSW–ENE direction, so that the maximum resistivity (B polarization mode) was assumed to be perpendicular to the PF.

The high frequency EM tomographic image shown in Fig. 7 has been carried out along the yellow profile 2 (Fig. 2) and, between measuring points 7 and 8, delineates a narrow vertical zone of resistivity associated to the PF.

3.3. Temporal distribution of the EM parameters related to geodynamic evolution of the slipping movement

As a first stage in getting to this aim, we used the magnetotelluric tensor impedance decomposition procedure (Bahr, 1988; Lilley, 1998) to identify the skewness and strike parameters carried out for the shallow structure. It is well known that skewness can be used as dimensionality parameter of the impedance tensor and it should be < 0.3 to interpret the structure as 2D. Thus, in our specific case, any changes of it in time can be associated with the ground motion occurred at certain depth interval. In the same manner, taking into account their theoretical interrelations (Bahr, 1988; Lilley, 1998), we have also used the anisotropy and strike parameters. At the micro-scale, the occurrence of the new cracks/micro-faults that are associated to the beginning of sliding processes may be reflected by the changes of the strike orientation.

The high frequency EM methodology and MAPROS software packages have been applied to reveal the landslide geodynamic evolution on the base of temporal variations of the skewness, strike and anisotropy parameters. Thus, at the intersection point of the both profiles 1 and 2 (green ring on Fig. 2) we carried out discrete measurements with a sampling rate of 7 days. The results are shown in Figs. 8, 9 and 10, pointing out the significant changes of the EM parameters, as follows:

– in the frequency range 2.10^3 – 4.10^3 Hz, specific to the sliding activity occurred in the depth interval 0–30 m, skewness parameter higher than 0.3 (Fig. 8) revealed a 3D structure (on 30th September), while the same structure becomes 2D on 07th October (when the skewness is smaller than 0.3);

– for the both records, the strike parameter (Fig. 9) has deviations of about 12^0 versus its mean value ($92^0 \pm 2^0$), which may be assigned to the new rupturing process/micro-fault having this orientation;

– in the same frequency ranges 2.10^3 – 4.10^3 Hz, the electrical anisotropy (Fig. 10) for rotated field is of about 1.8, on 30th September, and becomes of about 2.0–2.5, on 07th October.

4. LANDSLIDE HAZARD LEVEL ASSESSMENT

The approach developed for this study is based on the macrozonation methodology (Mora, Vahrson, 1994) that was adopted to be used for the available datasets. Thus, the landslide hazard level H is defined by a combination of susceptibility and triggering factors:

$$H = (Sr * Sl * Sh) * (Ts), \quad (7)$$

where:

– the intrinsic susceptibility factor is determined by multiplying the slope factor (Sr) with lithology factor (Sl) and relative soil moisture (humidity) factor (Sh);

– the triggering factor that initiates rapid movement and its probability of occurrence is given by the seismicity indicator (Ts).

By applying the equation (7) to the conditions of the Provița de Sus landslide, in order to determine the relative hazard level, it is obtained:

$$H\ landslide = (3 * 4 * 4) * (3) = 144, \quad (8)$$

where:

- Sr = 3 (the landslide slope angle is 18^0 and the classification of susceptibility is ***Medium***);
- Sl = 4 (the landslide lithology is represented by sedimentary rocks – Cenozoic, Quaternary and the classification of susceptibility is ***High***);
- Sh = 4 (in this study, soil humidity factor is correlated with **very low resistivity values of about 2–4 ohm.m,** obtained for the slide interface interval – Fig. 5 and the classification of susceptibility is ***High*);**
- Ts = 3 (Peak Ground Acceleration-PGA is between 101–150 cm/s^2 and classification of the seismic trigger indicator is 3).

As the value of relative landslide hazard level is **144**, according to classification presented in the frame of the macrozonation methodology (Mora, Vahrson, 1994), the landslide hazard potential is ***Moderate*** (class 3).

5. CONCLUSIONS

The described GBMS and methodology proved an effective way of monitoring the DC resistivity and high frequency EM parameters in order to detect their significant changes associated to the landslide Provița de Sus test-site. From these experimental data the following general conclusions can be drawn up:

1. The intermediate depth earthquake occurred on 27th, November 2004, in Vrancea zone, and the associated Provița fault were the major forces generating the beginning of the slide activity in Provița de Sus area.

2. The pattern of landslide induced by large (Mw = 6) earthquakes on the active fault Provița

is closely and quantifiably related to ground motion.

3. The significant post-seismic changes related to the morpho-geoelectrical features of the sliding interface, on the shallow depth interval (0–30 m), had only a local character, being mainly developed between the middle and front part of the landslide;

4. High-resolution of the EM parameters and tomographic images can lead to an improved understanding of landslide mechanism and hazard assessment due to both the seismic activity and active faults associated;

5. The changes of the EM parameters versus the geodynamic characteristics of the analysed test-site allowed us to consider the GBMS as powerful tool to investigate any landslide areas characterized by very complex geology;

6. The related study demonstrates the rich potential of using this new methodology for landslide monitoring. In particular, the GBMS and wireless connection for data transfer can play an important role in monitoring landslide-prone areas and in providing some useful data for a landslide hazard assessment – what might contribute to a better protection of the society.

Acknowledgements. This work was supported by CNCSIS-UEFISCSU, project number 1028/2009 PN II – IDEI code 14/2008.

REFERENCES

BAHR, K. (1988), *Interpretation of the magnetotelluric impedance tensor: regional induction and local telluric distortion*, J. Geophys., **62**, 119–127.

HAEBERLIN, Y.**,** TURBERG, P., RETIERE, A., SENEGAS, O., PARRIAUX, A. (2004), *Validation of Spot-5 satellite imagery for geological hazard identification and risk assessment for landslides, mud and debris flows in Maragalpa, Nicaragua*, The XXth ISPRS Congress, Commission I Papers, vol. XXXV, part B1, Int. Soc. Photogram. Remote Sens., Istanbul, Turkey, 2004.

HAVENITH, H-B., STROM, A., JONGMANS, D., ABDRAKHMATOV, K., DELVAUX, D., TREFOIS, P. (2003), *Seismic triggering of landslides, Part A: Field evidence from the Northern Tien Shan*, Natural Hazards and Earth System Sciences, **3**, 135–149.

LILLEY, F.E.M. (1998), *Magnetotelluric tensor decomposition: Part I, Theory for a basic procedure*, Geophysics, **63**, 6, 1885–1897.

MALET, J.P., MAQUAIRE, O, CALAIS, E. (2002), *The use of global positioning system techniques for the continuous monitoring of landslides: Application to the Super size Earth flow (Alpes-de-Haute-Provence, France)*, Geomorphology, **43**, 33–54.

McKEAN, J., ROERING, J. (2004), *Objective landslide detection and surface morphology mapping using high-resolution airborne laser altimetry*, Geomorphology, **57,** 331–351.

MEUNIER, P., HOVIUS, N., HAINES, A.J. (2007), *Regional patterns of earthquake-triggered landslides and their relation to ground motion*, Geophys. Res. Lett., **34**, L20408, doi: 10.1029/2007GL031337.

MORA, P., BALDI, P., CASULA, G., FABRIS, M., GHIROTI, M., MAZZINI, E., PESCI, A. (2003), *Global Positioning System and digital photogrammetry for the monitoring of mass movements: Application to the Ca' di Malta landslide (northern Apennines, Italy)*, Eng. Geol., **68**, (1–2), 103–121.

MORA, S., VAHRSON, W. (1994), *Macrozonation methodology for landslide hazard determination*, Bulletin of the Association of Engineering Geologists, **31** (1), 49–58.

ROKITIANSKY, I.I.**,** INGEROV, A.I. (2000), *Electrical studies of the Carpathian electrical conductivity anomaly*, Geophys. J., **19**, 793–810.

STĂNICĂ, D.**,** ZUGRĂVESCU, D. (2004), *Mobile geophysical laboratory: electromagnetic, electric and seismo-acustic analysis*, Studi Geologici Camerti, Special Issue, Active Faults: Analysis processes and monitoring, EDIMOND, Italy, 131–134.

STĂNICĂ, D., STĂNICĂ, M., VIŞAN, M. (2006), *Anomalous behavior of the electromagnetic parameters associated to intermediate depth earthquakes*. Rev. roum. Géophysique, **50**, 41– 47.

STĂNICĂ, D., STĂNICĂ, M. (2007), *Electromagnetic monitoring in geodynamic active areas*, Acta Geodinamica et Geomaterialia, **4**, 1(145), 99–107.

TATU, M., STĂNICĂ, D., POPESCU, M., MIREA, V. (2005), *Landslide hazard mapping in Romanian sub-Carpathians; Risk area estimation*. Abstracts Book at Technical Meetings of the Integrated Optimization of Landslide Alert Systems (OASYS)-EU FP5 Project, Modena, Italy, 3–4 February, 2005.

WANG, H.B., SASSA, K., XU, W.Y. (2007), *Analysis of a spatial distribution of landslides triggered by the 2004 Chuetsu earthquakes of Niigata Prefecture, Japan,* Natural Hazards, **41**, 1, 43–60.

WORD, R.D., SMITH, H.W., BOSTICK Jr., F.X. (1970), *An investigation of the magnetotelluric tensor impedance method*, Electronics Research Center, The University of Texas at Austin, Austin, Texas, 78712.

Received: July 28, 2010
Accepted for publication: September 17, 2010

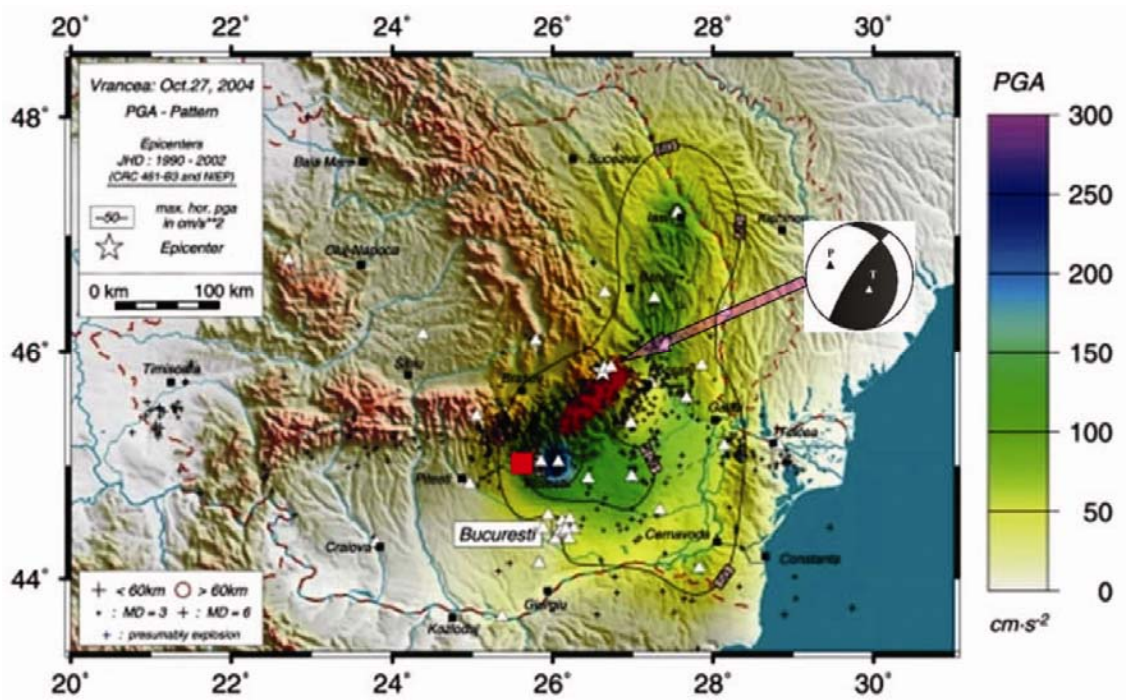

Fig. 1 – Provița de Sus landslide locations on the Romanian map (red rectangle) including the epicentre of the November 27th, 2004 Vrancea EQ (white star), PGA pattern (black isolines) and focal mechanism with fault plane solution oriented NE–SW (earthquake information after NIEP website).

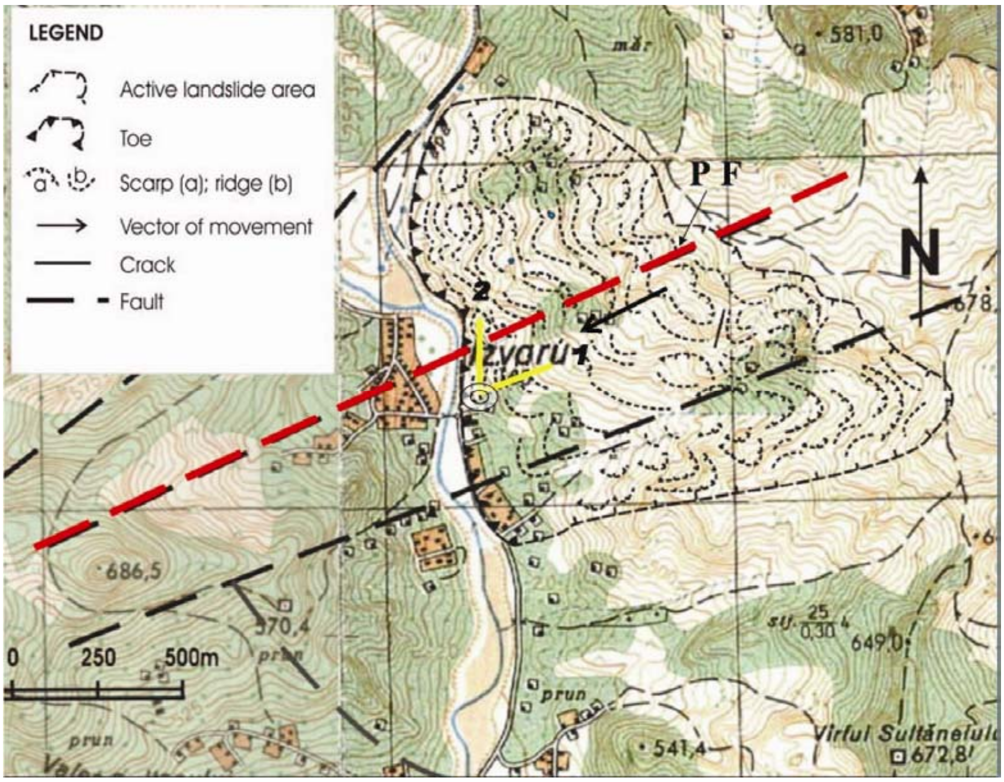

Fig. 2 – Provița de Sus landslide and PF (read dashed line) on the topographic map; the full yellow lines are DC resistivity and high frequency EM profiles; the white ring is measuring point of the high frequency EM parameters.

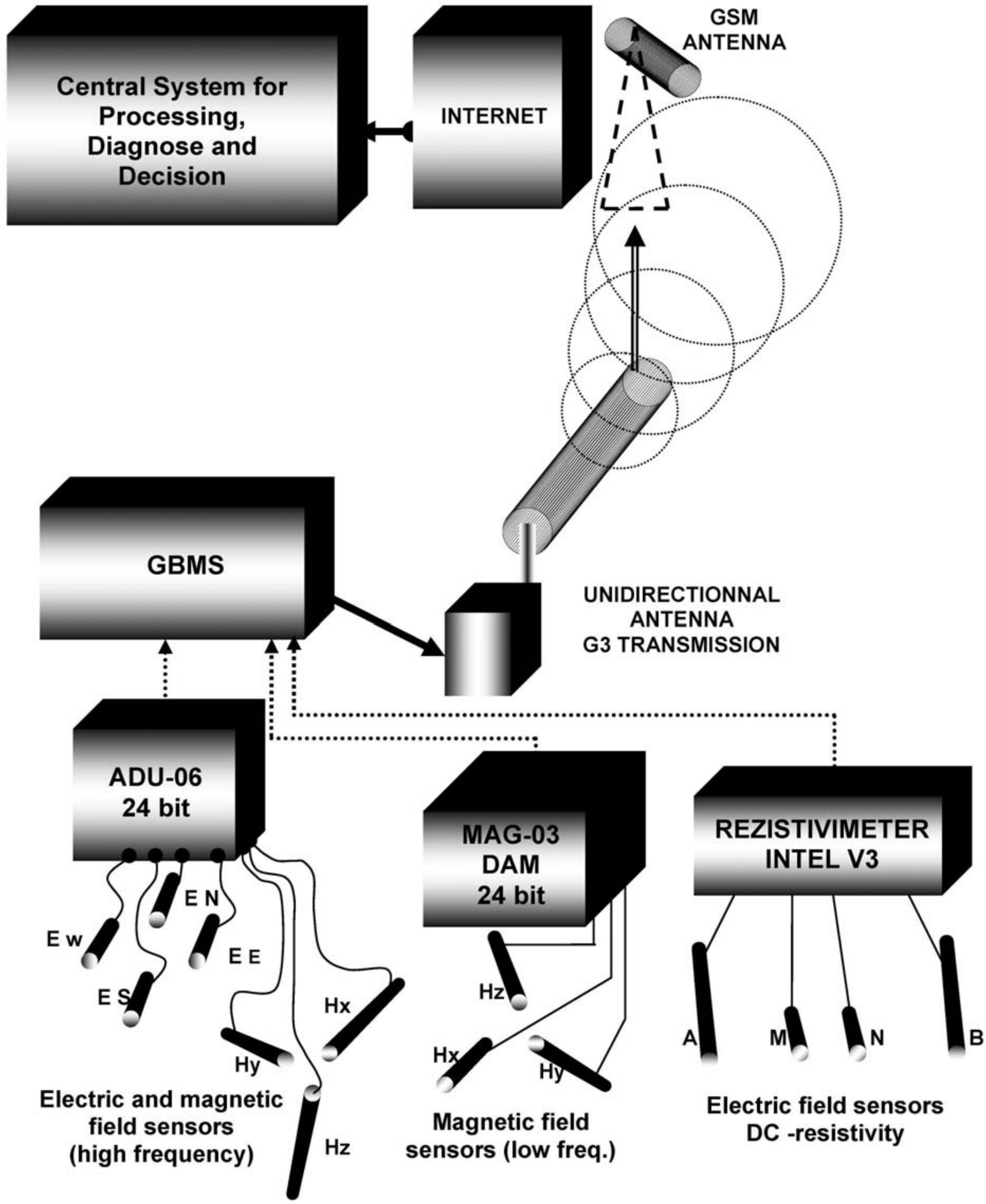

Fig. 3 – Ground-based monitoring system (GBMS) and wireless connection for data transfer.

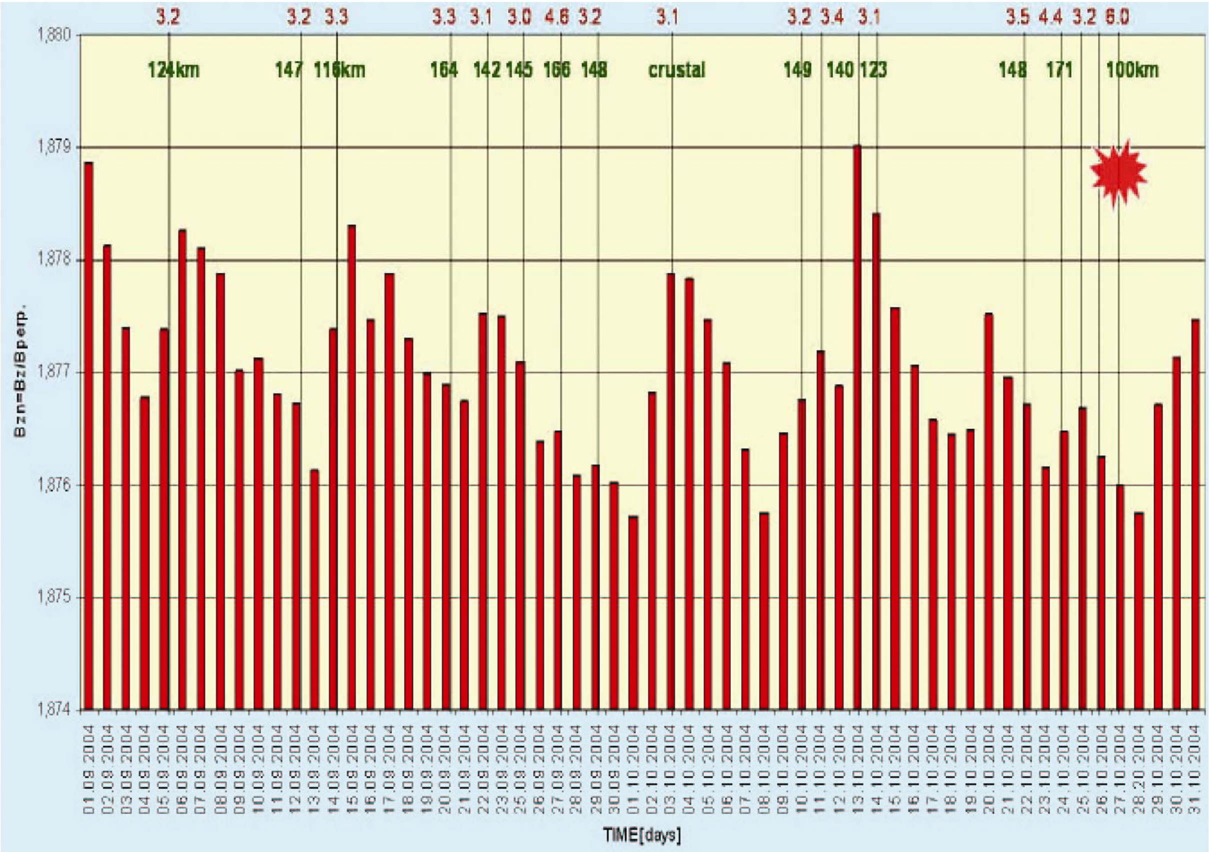

Fig. 4 – Daily mean distribution of the electromagnetic normalized function Bzn related to seismic events (vertical line) having marked their magnitude and hypocenter depth in km; red star marks the intermediate depth earthquake of Mw = 6.

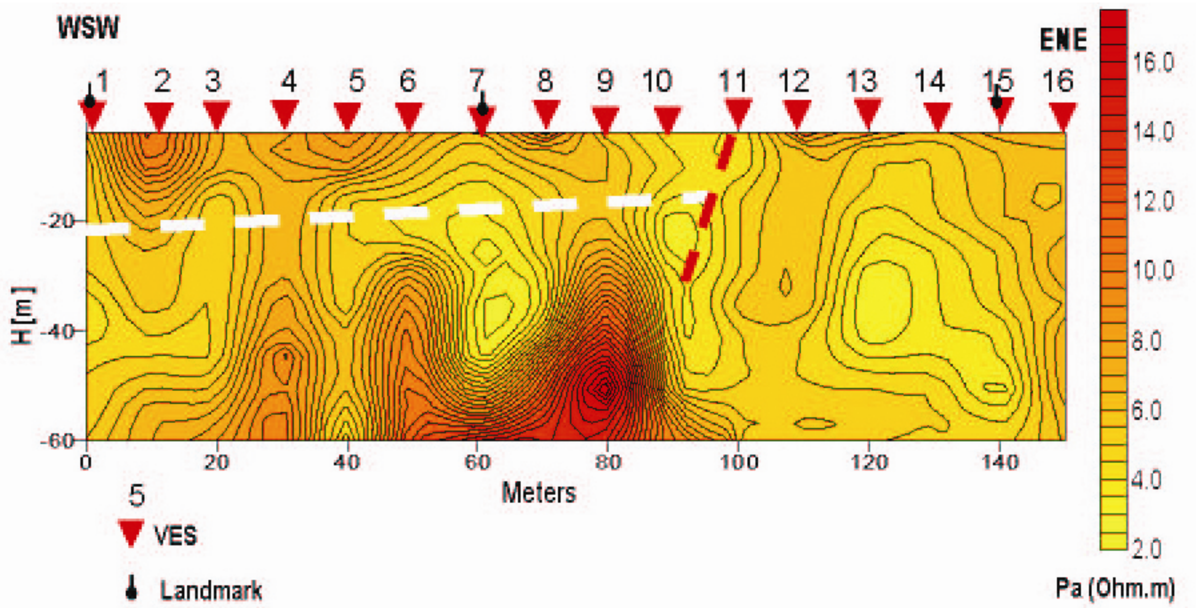

Fig. 5 – 2D resistivity image along the VES profile across the landslide zone (yellow line 1 on the Fig. 2); white and red dashed lines are the sliding surface and micro-fault, respectively.

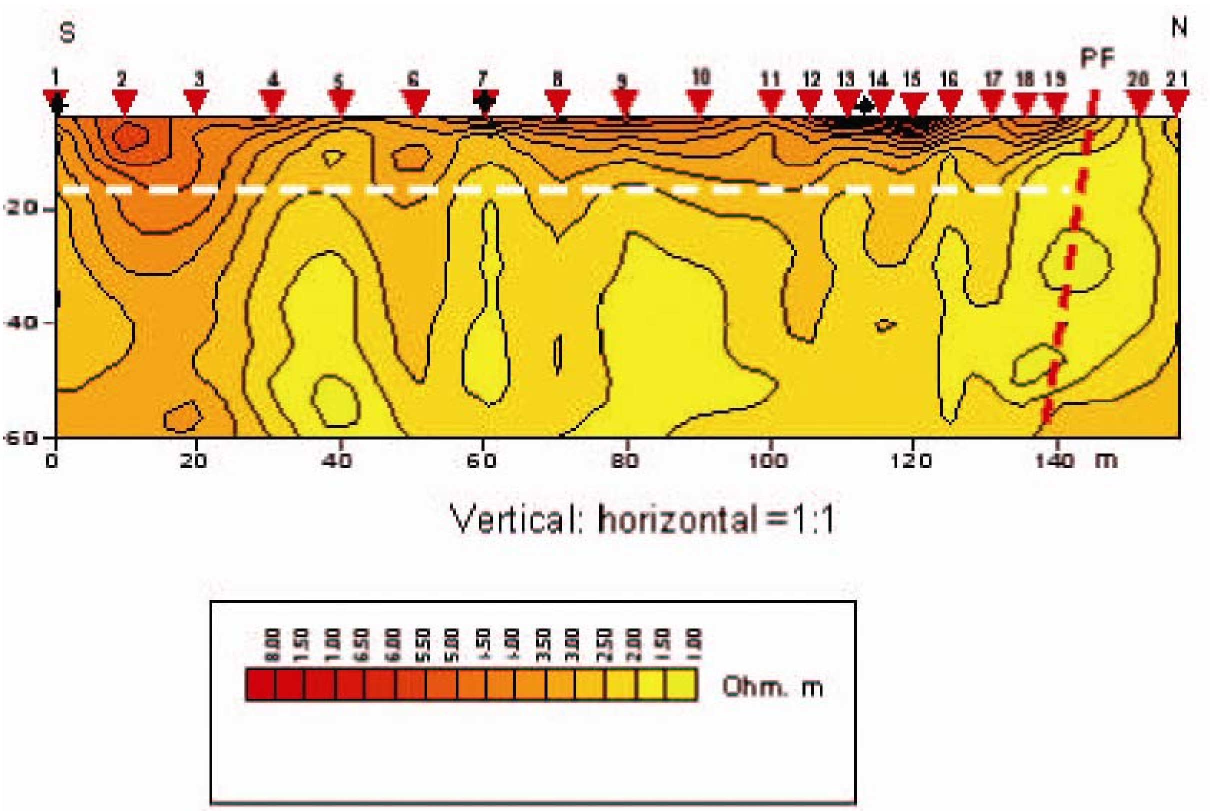

Fig. 6 – 2D resistivity image along the VES profile (yellow line 2 on the Fig. 2) showing the signature of the both sliding surface (white dashed line) and PF (red dashed line).

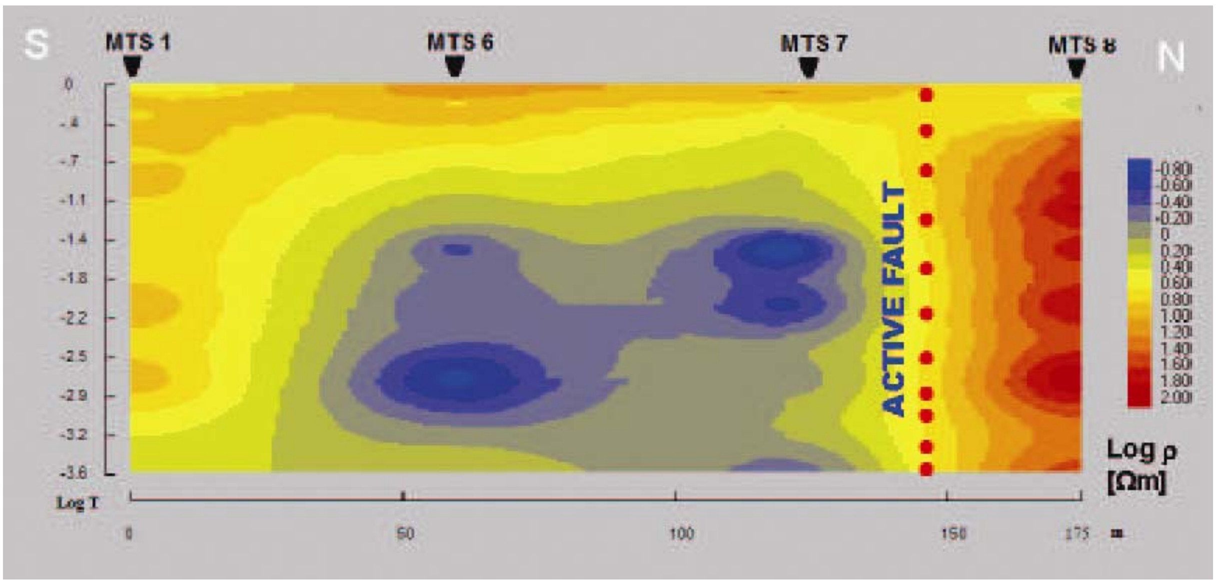

Fig. 7 – 2D high frequency EM image (B polarization mode).

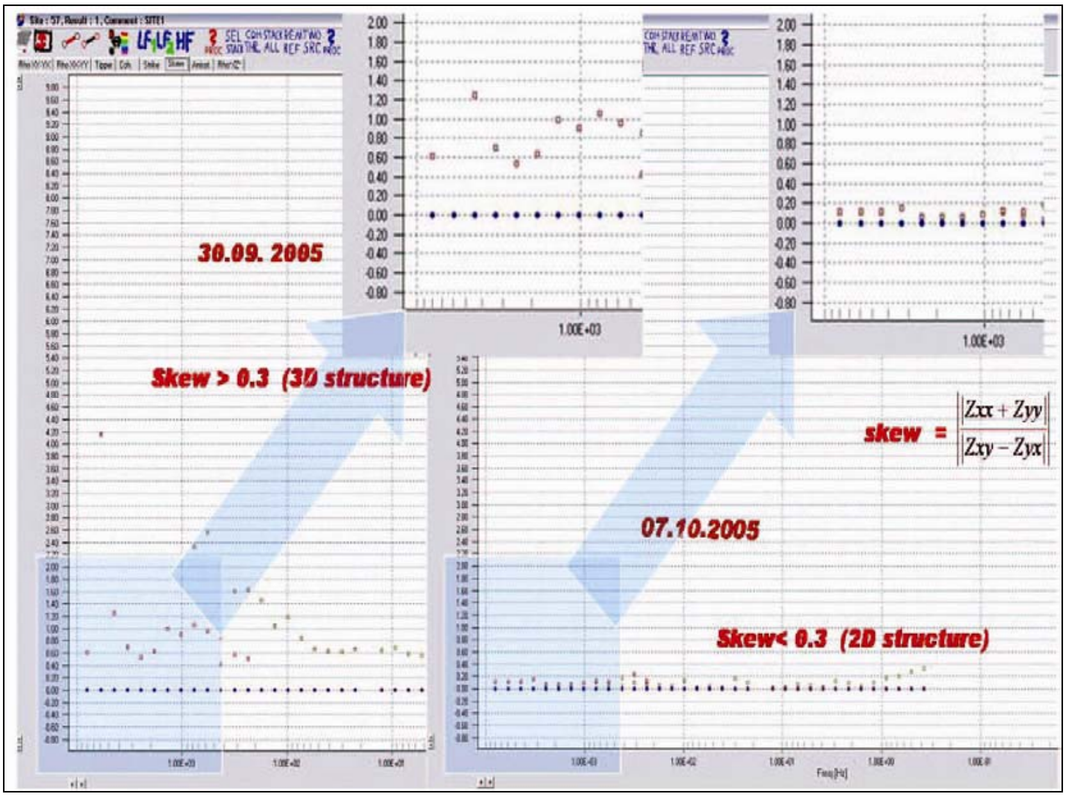

Fig. 8 – Skewness parameter recorded on 30th September, 2005 and 7th October, 2005.

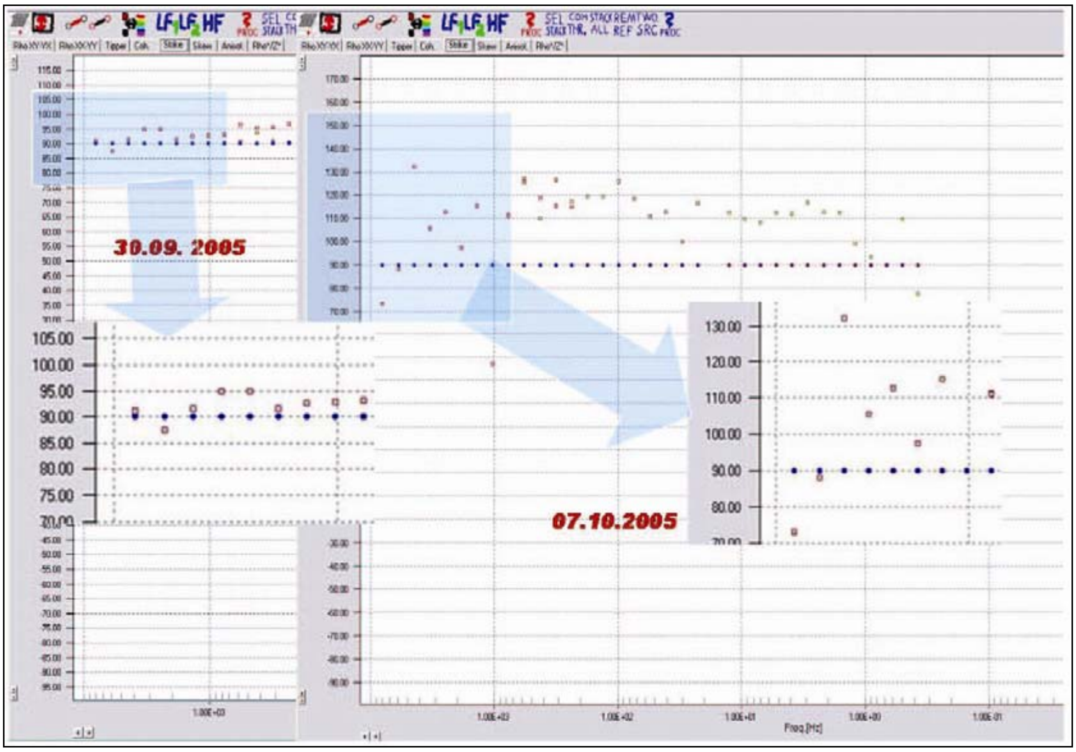

Fig. 9 – Strike parameter recorded on 30th September, 2005 and 7th October, 2005.

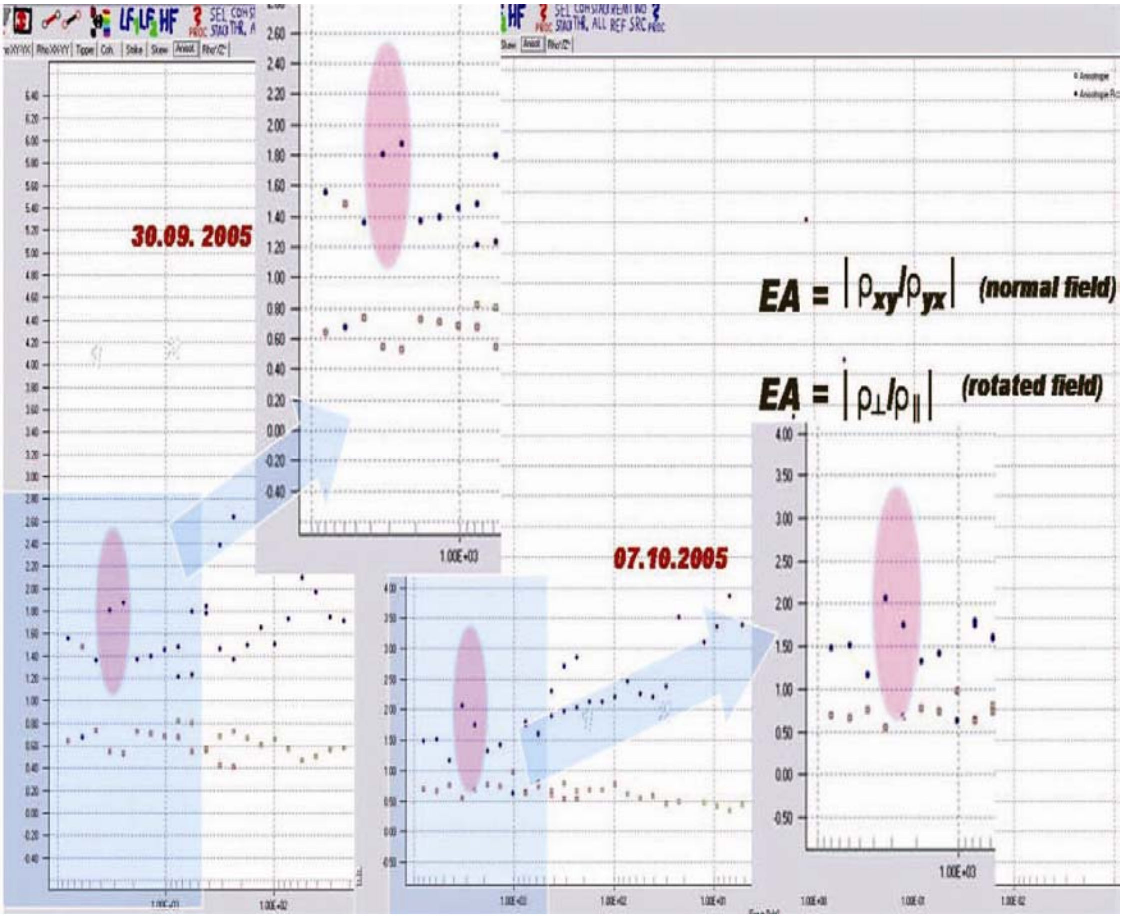

Fig. 10 – Electrical anisotropy (EA) recorded on 30th September, 2005 and 7th October, 2005; for normal and rotated fields; pink ellipse marks ground motion zone.